DEMONSTRATION AND EVALUATION OF THE Ka-BAND ARRAY FEED COMPENSATION SYSTEM ON THE 70-m ANTENNA

V. Vilnrotter and D. Fort

Submitted to TMOT Progress Report 42-139 (due Sept 1, 1999)

INTRODUCTION

The current plan for DSN evolution calls for the use of Ka-band (32 GHz) frequencies on large DSN antennas to increase antenna gain and useful communications bandwidth over that of current X- and S-band systems, with reduced sensitivity to plasma effects. However, there are a number of new problems associated with the use of higher carrier frequencies, including greater sensitivity to antenna deformations and misalignments, and more stringent pointing requirements due to narrower antenna beamwidths. Deformations and misalignments become increasingly problematic on the DSN's 70-meter antennas that are subject to severe gravitational stress, thermal gradients, focusing and other time-varying subreflector problems, vibrations induced by the mechanical drive-system, and by wind.

As the antenna tracks the target source (whether it is a spacecraft or a radio-source), time and elevation dependent loss components are introduced due to the Earth's rotation and due to the motion of the spacecraft, even in the absence of wind. The combination of these effects can lead to large losses from pointing errors and time-varying misalignments. Fortunately, most of these losses can be recovered by means of a properly designed compensation and tracking system that extracts the relevant deformation and pointing information from the received signal in real-time.

Real-time compensation for antenna deformations due to gravity, thermal effects and wind, together with accurate closed-loop tracking on 70-meter antennas will provide the DSN with greatly enhanced Ka-band capabilities for future missions: 8-10 dB gains over X-band on the 70-meter antennas, and up to 6 dB gain over 34-meter antennas are projected at Ka-band.

HISTORICAL BACKGROUND

An accepted technique for recovering losses due to gravitational deformations, thermal distortion and wind is by means of a real-time compensation system employing an array of feeds in the focal plane. The potential use of feed arrays for real-time compensation of antenna distortions and pointing applications has been extensively addressed in the literature starting as early as 1970 [1, 2, 3, 4].

A seven-element focal-plane array feed compensation system designed to recover gravitational and thermal losses on large DSN antennas has been constructed at the Jet Propulsion Laboratory and evaluated at the Goldstone complex. This system, called the "Array Feed Compensation System" (or AFCS) was developed to demonstrate real-time gravity-compensation and closed-loop tracking of both spacecraft and radio-sources at Ka-band frequencies. Both of these concepts have been successfully demonstrated in the pedestal-room of the 34-m Beam Waveguide Antenna at DSS-13 between 1995 and 1998, using spacecraft (SURFSAT, MGS) as well as radio-sources (planets and quasars). These initial concept demonstrations on the 34-meter antenna were followed by experiments on the 70-meter antenna at DSS-14, including joint AFCS plus Deformable Flat Plate (DFP) demonstrations on the 70-meter antenna. In this experiment, the DFP functioned as a controllable RF reflector surface placed in front of the AFCS in order to refocus divergent RF fields into the array.

Compensation and tracking on the 70-meter antenna is much more challenging than on 34-meter antennas due to greater gravitational deformations and greater vulnerability to thermal gradients and wind. Following successful compensation and tracking demonstrations on the 34-meter Beam Waveguide Antenna at DSS-13, the AFCS was moved to DSS-14 and installed on the XKR-cone of the 70-meter antenna for experimental testing and demonstrations – later, the XKR cone was removed for upgrades, during which time the AFCS, the DFP and a Ku-band (12 GHz) holography receiver were installed in the refurbished holography-cone, which was then mounted on the 70-meter antenna in place of the XKR-cone. For the following three and a half months (from mid-November through February) a series of experiments (called the "holography-cone experiments") were carried out to demonstrate and evaluate various candidate Ka-band gravity-compensation and tracking systems proposed for the DSN. Here we concentrate on the AFCS results, but also describe the joint AFCS/DFP experiment carried out the last day before the holography-cone was removed.

THEORETICAL BACKGROUND

The recently concluded "holography-cone experiments" attempted to characterize, evaluate and compare candidate breadboard systems designed to improve Ka-band performance of the DSN's 70-meter antennas by means of active gravity compensation and closed-loop tracking. Both the AFCS and the DFP were tested separately at virtually all elevations of interest (from 6 to nearly 85 degrees elevation): in addition, these two systems were also tested jointly on DOY-056, where the role of the DFP was to refocus divergent rays back into the array, while the AFCS combined the collected signal fields optimally in real-time in order to maximize the received SNR.

Due to severe time-constraints, only the lower range of elevations could be investigated with the joint configuration, covering elevations from slightly above the rigging angle (about 50 deg. elevation) down to nearly the software limit of the antenna (8.5 deg.). Analysis of this data demonstrated that a joint Ka-band AFCS/DFP compensation system working together in real-time could recover virtually all of the signal energy lost to gravitational deformation at intermediate to low elevations, effectively synthesizing an undistorted 70-meter antenna at Ka-band frequencies.

In order to meet operational requirements, a practical gravity compensation system (such as the AFCS, or a joint AFCS/DFP system) needs to perform two distinct tasks simultaneously: dynamic compensation for deformations due to gravity, thermal gradients and wind, and real-time estimation of the "best" pointing offset in order to maximize the combined SNR. The details of these operations are discussed in greater detail in the following sections.

1. Deformation Compensation

The DSN's 70-meter antennas were originally designed to receive S-band (2 GHz), and later expanded and improved to enable efficient reception of X-band (8 GHz) frequencies. At these relatively long wavelengths structural deformations did not create a serious problem. However, at the much shorter Ka-band (32 GHz) wavelengths planned for the future, deformations of the antenna structure due to gravity, thermal gradients and wind lead to unacceptable losses, particularly at very high and very low elevations. It has been determined experimentally that with conventional single-horn Ka-band receivers SNR losses on the 70-meter antenna at DSS-14 approach 4 dB at the lowest elevations, and often exceed 8 dB relative to the antenna's peak response at elevations above 80 degrees. These losses must be greatly reduced before 70-meter antennas can be gainfully employed for operational reception of Ka-band signals.

The theoretical framework for optimal real-time combining of signals from several different horns in order to recover SNR, has been detailed in several papers [5, 6, 7]. It has been shown that for a given signal vector and arbitrary noise variance in each channel, the combining weights that maximize the SNR of the combined channel are given by the expression

$$\tilde{w}_k = \frac{\tilde{S}_k^*}{\sigma_k^2} \tag{1}$$

where $\tilde{S}_k$ is the signal amplitude in the k-th channel, σ_k^2 is the variance of the noise, tilde denotes a complex quantity, and asterisk refers to complex conjugation. The optimally weighted combined digital signal samples can be expressed as

$$\tilde{z}(i) = \sum_{k=1}^{K} \tilde{r}_k(i)\tilde{w}_k \quad \text{where the received noisy samples are} \quad \tilde{r}_k(i) = \tilde{s}_k(i) + \tilde{n}_k(i) \tag{2}$$

and the index "i" refers to time. The "signal-to-noise ratio" of the combined sequence, denoted as SNR_c, is defined as the average power in the weighted signal divided by the average power of the weighted noise:

$$SNR_c = \frac{\left|\sum_{k=1}^{K} \tilde{S}_k \tilde{w}_k\right|^2}{\sum_{k=1}^{K} |\tilde{w}_k|^2 \sigma_k^2} = \sum_{k=1}^{K} \frac{|\tilde{S}_k|^2}{\sigma_k^2} \tag{3}$$

This expression shows that the SNR of the optimally combined signals is equal to the sum of the individual channel SNR-s. Inherent in this result is the assumption that the combining weights are known exactly, a condition that typically cannot be achieved in practice since the combining weights must be estimated from imperfect real-time measurements of signal and noise parameters. However, when observing strong and stable Ka-band signals the combining weights can generally be determined with sufficient accuracy to validate the assumption of perfect weight estimates. Alternately, a straightforward approach to determining the SNR of the combined channel is to measure it directly from the combined samples: both of these approaches were employed simultaneously by the AFCS digital signal processing assembly to help confirm the accuracy of the measurements.

2. Antenna Pointing and Tracking

Functional requirements for collecting experimental data, and for operational reception of spacecraft telemetry are typically very different. Experimental data is collected using a closed-loop "boresighting" algorithm: this is a "direct measurement" algorithm that determines the direction to the peak of the gain pattern by measuring the signal power at several points near the peak, and interpolating the results. This approach is well-understood and yields accurate results when performed under stable observing conditions, but requires serial measurements of "off-source" points to trace out the power-distribution, hence introduces an inherent SNR variation into the signal. While this is acceptable for experimental data-gathering, it is not desirable for telemetry reception where unwanted SNR variations degrade the decoding of the data. In addition, the serial nature of the measurements can lead to pointing errors if there happens to be significant temporal variation in spacecraft power, as often occurs during orbital maneuvers or when ranging-pulses are employed. For these reasons, the Array Feed "inferred measurement" tracking algorithm is preferred for operational use, since this algorithm determines the best pointing direction entirely from parallel measurements on the array channels.

The "inferred measurement" tracking algorithm uses simultaneous measurements of the signal in all seven channels, without ever pointing the antenna off-source as must be done with conventional "boresighting" or CONSCAN techniques. Although this tracking algorithm could not be fully demonstrated during the recently concluded "holography-cone" experiments due to lack of time, very high-quality data was obtained from the DS1 spacecraft which can be used to develop and improve the tracking algorithm, as well as simulate its performance on the real antenna.

AFCS DESIGN

A block diagram of the Array Feed Compensation System (AFCS) used in the recently concluded holography cone experiments is shown in Fig. 1. This system is essentially identical to the one evaluated on the XKR-cone of the 70-meter antenna at DSS-14, and previously in the pedestal room of the 34-meter antenna at DSS-13. The entire system can be conveniently separated into two major sections, an "Analog Front-End" (AFE) and a "Digital Signal Processing Assembly" (DSPA). The AFE consists of a seven horn feed array, cryogenically cooled HEMT low-noise amplifiers, and a seven channel downconverter assembly that translates the received signal from Ka-band to nominal 300 MHz IF. The DSPA further downconverts the IF signal to complex baseband, where it is sampled and combined, using real-time estimates to compute the optimum combining weights. Digital algorithms are employed to extract the pointing information from the signal, which can then be used to keep the antenna pointed on-source.

1. Array Feed Front End

The feed array consists of seven identical smooth-walled Potter horns, each 1 ¾ inches in diameter, providing 22 dBi gain at 32 GHz. The wall of each horn is tapered near the top to facilitate close packing, thus minimizing the loss of signal energy between the horns. The cryogenic front-end contains circular-to-rectangular waveguide transitions, polarizers, 20-dB couplers for each channel to enable externalnoise diode and tone inputs for calibration, three-stage HEMT low-noise amplifiers (LNA-s) that provide nominally 25 dBi of gain, thus establishing high SNR without adding significant receiver noise to the signal; and thermal components such as a heat-sink and a "charcoal trap" to gather up the remaining molecules and thus help produce a better vacuum. The output of each HEMT LNA is an amplified RF signal at 32 GHz nominal center frequency. Next, the seven RF signals are translated to 300 MHz intermediate frequency (IF) by the Seven Channel Downconverter Assembly and transmitted via seven coaxial IF cables to the DSPA, located in the alidade of the 70-meter antenna.

In the alidade, the seven IF signals are processed by an IF-to-baseband downconverter assembly, which shifts the signals from 300 MHz (nominal center frequency) to a video frequency within the passband of the digital system. Both in-phase and quadrature components are extracted from the IF signals, downconverted to a "baseband video center frequency" of approximately +20 KHz (default, manually resettable), sampled using a bank of fourteen analog-to-digital converters (ADC-s) and thus converted to complex digital samples. From this point on, the digital processing depends on the type of source being observed. The DSPA has been designed to process either broadband sources (radio sources such as quasars and planets), or narrowband sources such as that produced by the residual carrier of a Ka-band spacecraft. Either approach can be selected by the user: in each case the final result is a "combined channel" output with maximized SNR, although different techniques must be employed to estimate the optimum combining weights for the two cases. In addition, the DSPA also extracts pointing information from the complex baseband samples, thus providing an option to update the antenna's predict-driven "blind pointing" algorithm with closed-loop tracking based on real-time pointing information: the user can choose between broadband and narrowband versions of an accurate and well-tested AFCS "boresighting algorithm" or the experimental "inferred-measurement tracking algorithm" described above.

2. Digital Signal Processing Assembly (DSPA)

The DSPA uses four TMS320C40 floating point processors operating at 50 MHz and connected in a circular chain, located on signal processing boards within the PC. The incoming data is sampled continuously with 16-bit resolution at 96000 samples per second and stored in 750-sample buffers by the first processor, then shifted from processor to processor until finally the combined data is added into the buffer. The first processor then sends the combined channel samples to the digital-to-analog converters. The second processor removes any DC offsets from the samples and scales the data using parameters obtained from the PC (either user input or stored). The third processor produces the combined channel samples using complex weights obtained from the PC, and puts the result in the buffer as the 'eighth' channel. The fourth DSP processes all eight feeds as instructed by the PC, and

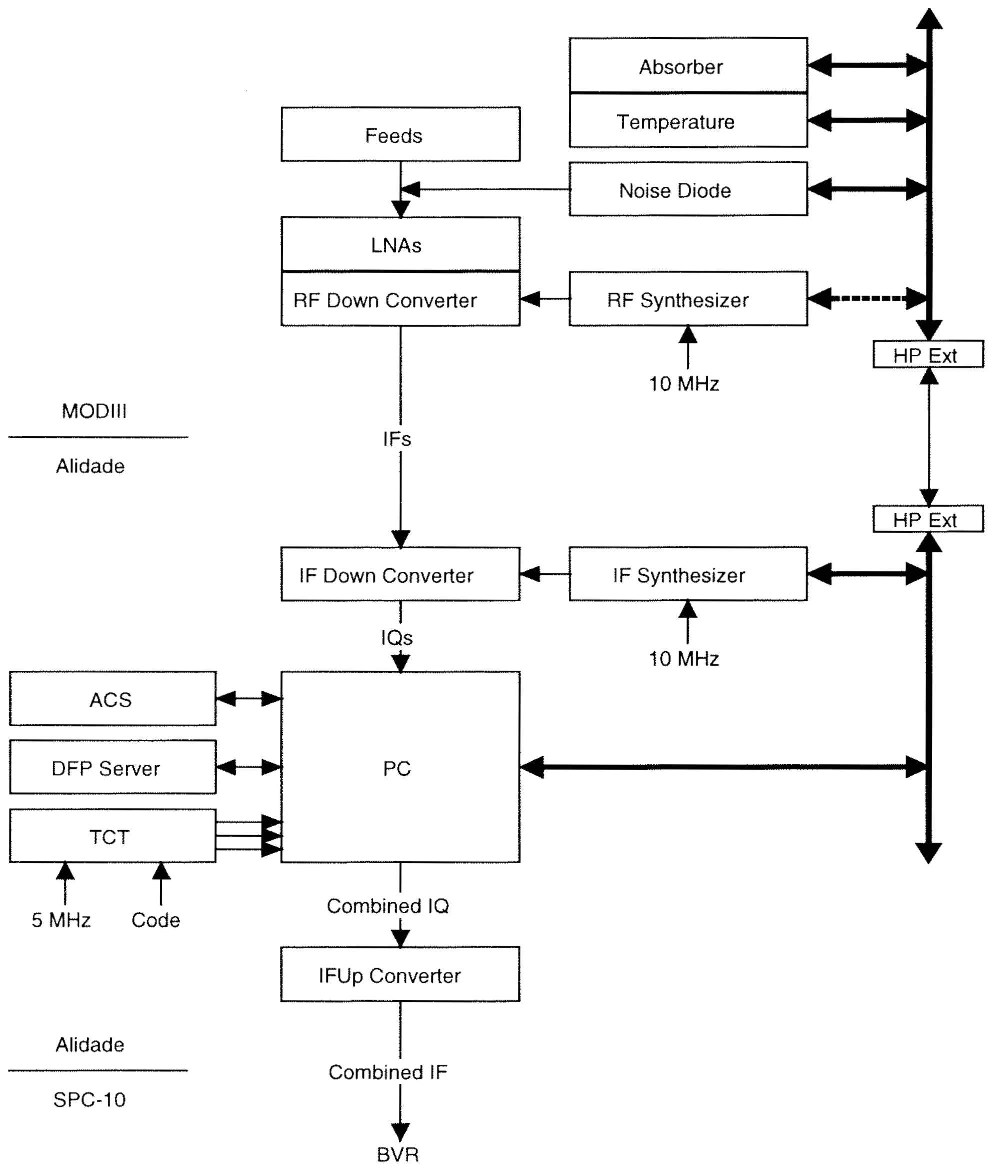

Fig. 1a Array Feed Compensation System Block Diagram

sends the results (eight complex numbers) to the PC for processing or output 128 times a second (note that 128 x 750 = 96000). The operations performed by the fourth processor on demand are:

1 - return the first sample in the buffer - used for diagnostic purposes
2 - return the sum of all samples - used for calibrating DC offsets
3 - return the sum of squares of all samples - used for power measurements
4 - return the cross correlation of each channel with the central channel - used for calculating the
combining weights for broadband sources (quasars).
5 - return the sum of the samples rotated by a phase model supplied by the PC - used for calculating the weights for narrow band sources (spacecraft).

The PC is used for both control and data processing, and incorporates a real-time operating system (RT-KERNEL). Data processing includes reading time from the TCT (Time Code Translator) and responding to 1 PPS and 100 PPS interrupts generated by the TCT. DC offsets and gains are calculated and sent to the DSP subsystem when requested by the user (these offsets and gains change very slowly, if at all). When observing spacecraft, carrier frequency predicts are generated from normal NSS predict files and the carrier frequency sent to the DSP subsystem 128 times a second. Correlation and rotation results are used to derive the complex weights via a Fourier transform technique, and downloaded to the DSP subsystem periodically. The power measurements are also used to perform conventional system calibrations with noise diode and absorber.

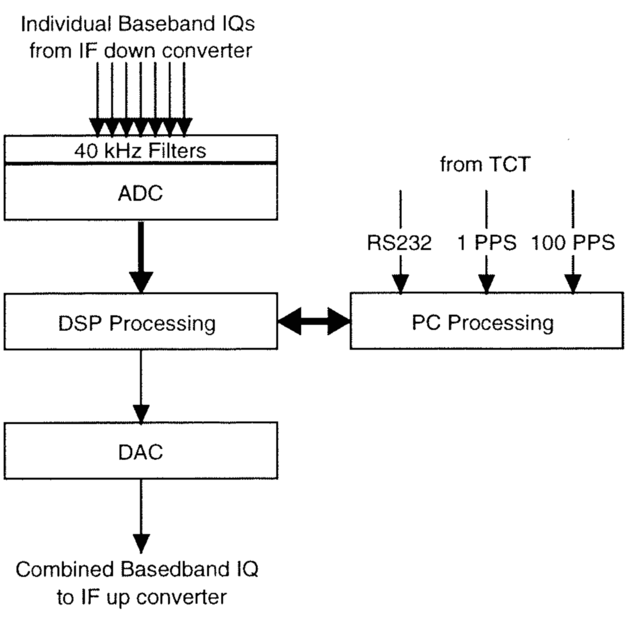

Fig. 1b AFCS Digital Signal Processing Assembly (resides in PC)

EFFICIENCY MEASUREMENTS

Single-horn antenna efficiency measurements were carried out using the central channel of the AFCS. These were based on simultaneous power meaurements of the Ka-band calibrator 3C274 by: a) the digital power meter incorporated into the DSPA, and b) analog power measurements using a calibrated HP power meter connected directly to the IF of the central channel. Source power was measured on three separate occasions near the rigging angle under good atmospheric conditions (clear, calm weather): the power readings were averaged, and the average elevation of the three measurements computed. Antenna efficiency at each elevation was estimated by dividing the average temperature of the source (T_{src}) by the value published for 3C274 in [8] for a 100 percent efficient antenna (T_a=11.9 kelvins). The results of these measurements are:

DOY	Elevation	T_{src}	Efficiency
011	45 deg	3.8 K	31.9%
035	41 deg	3.1 K	26.1%
038	45.4 deg	3.6 K	30.4%

The average efficiency was found to be 29.4% at an average elevation of 43.8 degrees.

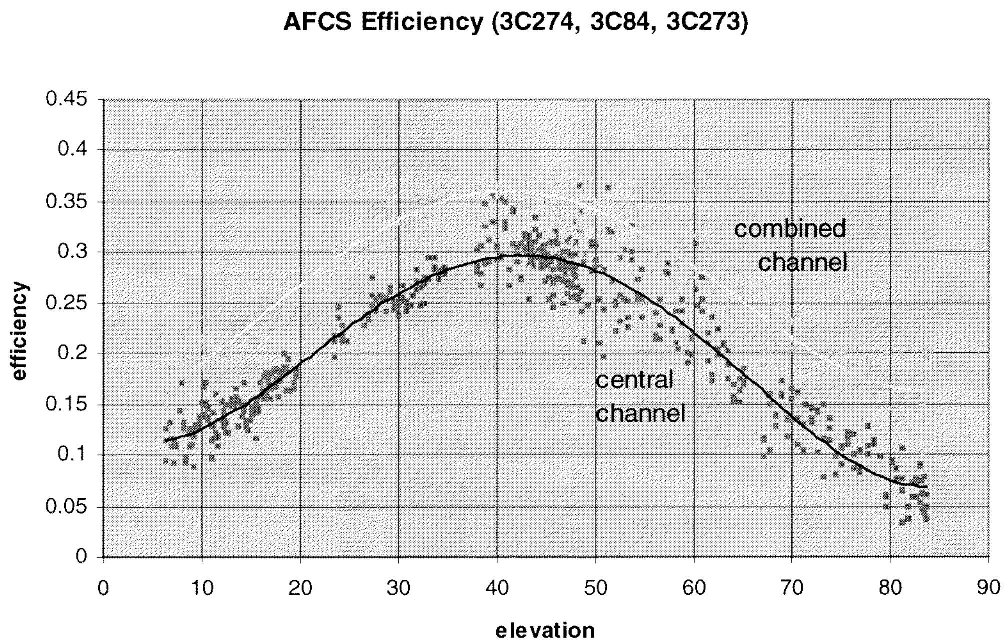

Fig. 2 Efficiency curve of the 70-m antenna; AFCS central channel (not corrected for atmospheric effects)

The source power was also measured simultaneously using digital techniques and compared to the HP measurements, which was taken as the reference. The scale factors thus derived were transferred to the digital power measurements of other radio sources that were also for efficiency measurements, namely 3C273 and 3C84, when these sources were near the rigging angle. Thus, an estimate of antenna efficiency as a function of elevation was obtained over an elevation range of 6 to 84 degrees. Since the power in all seven channels was recorded by the DSPA on every track, this information was also used to measure the efficiency improvement provided by the array ("combined channel" data in Fig. 2).

Analysis of the 4-th order polynomial fit to the central channel data in Fig. 2 indicates that at very low elevations (near 6 degrees) the central channel efficiency drops to about 11%, representing an efficiency loss of 4.3 dB, while at very high elevations (84 degrees) the measured efficiency drops to 7%, representing a loss of 6.2 dB from peak response. Similarly, analysis of the 4-th order fit to the combined channel data indicates a peak response of 36% near 42 degrees elevation, with low and high elevation efficiencies of 17%, representing losses of 3.25 dB at the extreme elevations. Note that this data has not been corrected for atmospheric extinction, which is most prominent at low elevations: using the measured value for zenith extinction of 0.1 dB (corresponding to one air-mass), the correction for lower elevations can be found by determining the number of air-masses at the elevation of interest (using "number of air masses" $= 1/\sin(\theta)$). Thus, the attenuation at 6 degrees elevation is 0.1/sin(6 deg) = 0.96 dB, or a factor of 1.25, hence both central and combined channel efficiencies have to be increased by this amount, yielding 13.7% and 21.2% respectively for the corrected central and combined channel efficiencies. Ignoring the small correction due to the slight increase in air mass at the rigging angle and above, this implies that the corrected efficiency loss for the central channel at 6 degrees elevation is 3.3 dB, while that of the corrected combined channel is 2.3 dB. Taking the ratios of combined to central channel efficiencies, the combining gains estimated from this data are 1.9 dB, 0.87 dB and 3.8 dB at 6 degrees, 42 degrees and 84 degrees respectively.

ARRAY FEED COMPENSATION SYSTEM

1. Combining

The "New Millenium" spacecraft DS1 provided a stable Ka-band signal throughout the holography cone experiments. After its Ka-band transmitter was turned on, DS1 produced a strong Ka-band signal which usually contained a significant "residual carrier" component whose power depended on the modulation index. There were two modes of operation for Ka-band downlink: "one-way" and "two-way" modes. In one-way mode, the spacecraft's on-board oscillator was used to generate the carrier signal, while in two-way mode a highly stable frequency reference was transmitted up to the spacecraft from the ground which the spacecraft oscillator used as reference, modulated, and retransmitted to the ground.

A typical DS1 data-gathering track consisted of the following steps: 1. frequency and pointing predicts were obtained and supplied to SPC-10; 2. the antenna was "blind pointed" towards the spacecraft and the frequency predicts were used to acquire the residual carrier; 3. the residual carrier was downconverted into the passband of the DSPA (nominally 20 KHz), integration time and loop gain were set (minimum of 1 sec integration time with current architecture) and the frequency tracking loops were locked up; 4. a "boresighting" sequence was initiated to refine antenna pointing in order to peak up the signal; 5. data gathering or other pertinent experiments commenced.

Most of the time spent during a typical DS1 track was allocated to collecting combining data over a range of elevations. Since the antenna tends to exhibit considerable drift from the pointing model (particularly at low and high elevations), it was necessary to update the antenna pointing in real time: this was accomplished using the coherent version of the Array Feed boresighting algorithm. The array feed boresighting algorithm applies small positive and negative pointing offsets from the nominal "on-source" direction along both the elevation and cross-elevation axes, measures the signal power at each offset (including the nominal "on-source" direction), and estimates the direction to the peak from a quadratic fit to the data. The algorithm records the complex signal voltage at the end of each integration time, measures the rms noise voltage, and updates the optimum combining weights in all seven channels. It also measures and records the complex signal voltage and rms noise voltage in the optimally combined channel. This information can be used to determine the SNR in the combined channel directly. Dividing the SNR of the combined channel by that of the central channel yields the "combining gain" of the AFCS, formally defined as

$$Combining\ Gain; \quad G_c \equiv \frac{SNR\ of\ combined\ channel}{SNR\ of\ central\ channel} \tag{4}$$

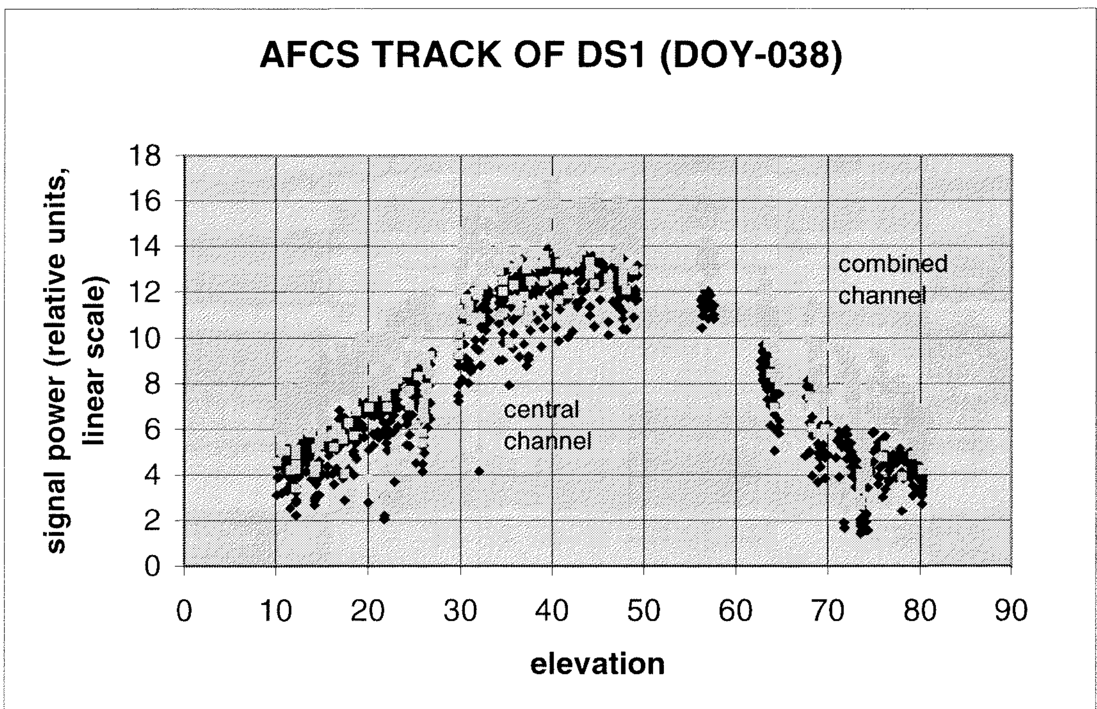

Fig. 3a DS1 Signal Power as a Function of Elevation

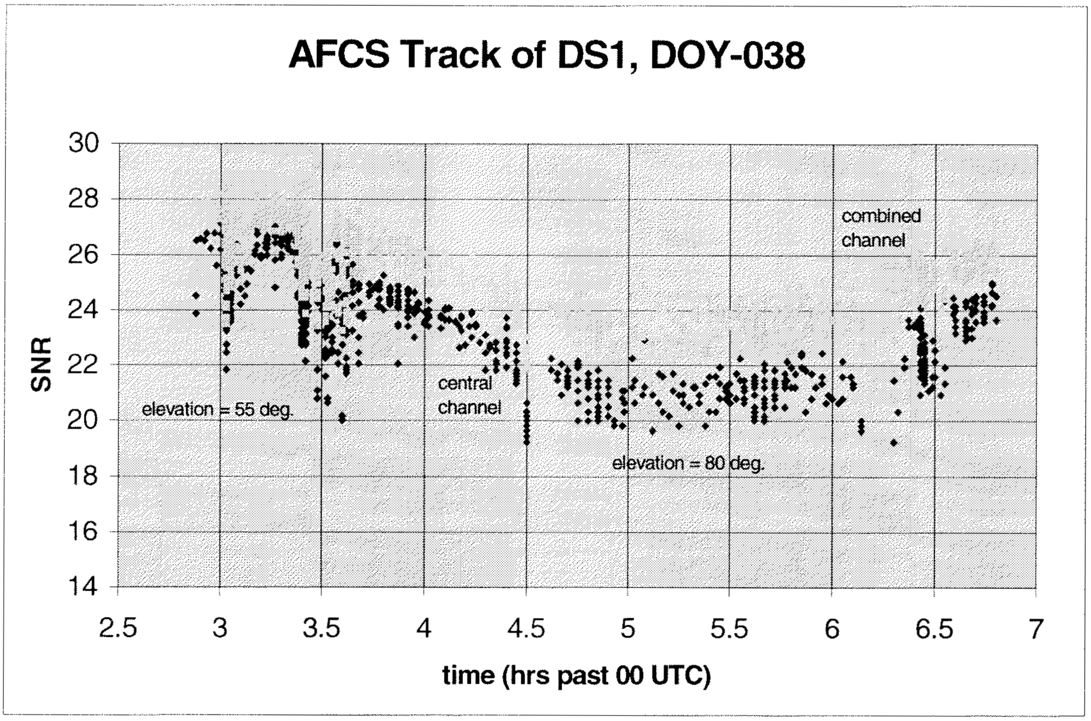

Fig. 3b DS1 Signal Power as a Function of Time

Data collected on DOY-038 is displayed two different ways in Figures 3a and 3b: the first shows signal power as a function of elevation on a linear scale to facilitate comparison with the efficiency curve of Fig. 2, while the second shows SNR in dB as a function of time. The compensating effect of the AFCS is most clearly demonstrated in Fig. 3b, where the SNR loss at high elevation, as the antenna tracks the source through transit, is significantly less in the combined channel than in the central channel: at high elevations the combining gain is seen to be approximately 3 dB, yielding a less severe SNR drop than in the uncompensated central channel.

Combining gain was found to be a very useful quantity for evaluating AFCS performance, since it is not affected by perturbations that are common to all seven channels at the same time: for example, it was found that the relatively long, one second integration time employed by the current DSPA architecture produced an effective frequency tracking loop bandwidth that was too narrow to track the phase dynamics of the received signal accurately, resulting in simultaneous "signal fades" in all seven channels. This caused large scatter in the SNR of each channel, as well as of the combined channel, as evident in Figs. 3a and 3b. However, since the "random fading coefficients" were identical in both the combined and central channels, taking the ratio as in (4) lead to cancellation of the fade coefficients regardless of their instantaneous value, resulting in much more accurate estimates of combining gain.

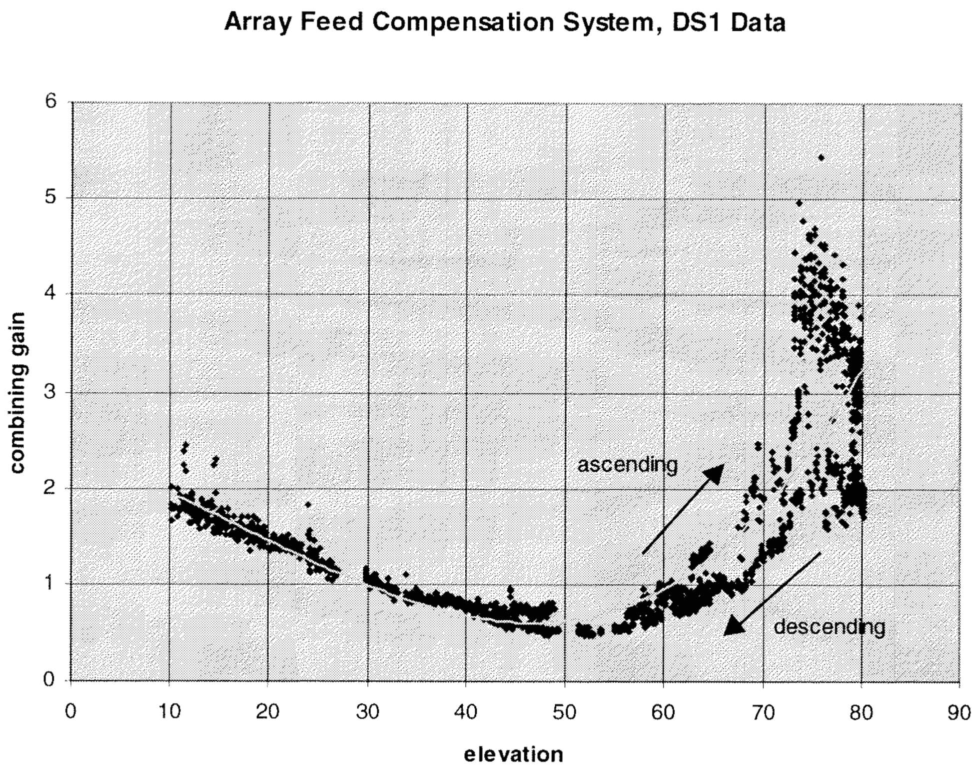

Fig. 4 Composite Array Feed Combining Gain as a function of Elevation

The improvement in the combining gain data is clearly illustrated in Fig.4, where the data exhibits much less scatter (or, the implied "error bars" are much smaller) than for the original SNR data. Note that above 60 degrees elevation the data appears to split into two distinct branches, indicating an azimuth dependence in the combining gain: the upper branch corresponds to the ascending part of the track (before transit) while the lower branch corresponds to descent towards the horizon (after transit). This asymmetrical behavior of the antenna has been observed on all occasions, but the exact cause is not well understood at this time.

Consistent with previous analyses of both radio sources and DS1 data, the combining at low elevations is seen to approach 2 dB, dropping to less than 1 dB near the rigging angle, and increasing to as much as 4 dB around 75 degrees ascending, 3 dB near transit, and little over 2 dB around 75 degrees descending. The third-order trendline indicates average gain at a given elevation, without taking into account the azimuth dependence of the gain curve at high elevations.

2. Tracking

A very accurate "direct measurement" boresighting algorithm that works with broadband sources as well as coherent tones has been developed and installed into the AFCS before the start of the holography cone experiments, and has been used throughout to provide closed-loop pointing of the antenna. This algorithm relies on the periodic introduction of small pointing offsets to estimate the direction of the signal-peak, which unfortunately results in unavoidable SNR-loss when the antenna is pointing off-source. In addition, the inherent serial nature of the measurements makes it vulnerable to errors due to variations in signal power or changes in atmospheric conditions during the measurement. The "inferred measurement" algorithm currently being developed uses simultaneous measurements of the signal in all seven channels, without the need to point the antenna off-source, thus it is immune to signal power variations and does not degrade the SNR of the signal. Due to time-constraints during the holography-cone experiments, all of the tasks proposed in the original (very ambitious) experiment plan could not be addressed: in particular, the development and demonstration of the inferred measurement algorithm could not be completed. However, very high quality data was obtained from tracking the DS1 spacecraft, which was near the earth during this time and hence provided a strong and stable signal.

Since the feed array can be viewed as an instrument for obtaining samples of the focal-plane field distribution, it should be possible to extract accurate pointing information from these samples in real time, even in the presence of severe antenna distortions. This hypothesis was tested during the holography cone experiments by measuring and recording the complex array response for a raster of small offsets from the optimum pointing direction at 10 degree elevation increments, while tracking DS1. The "raster model" thus compiled effectively characterized the effects of antenna distortion at all elevations, and simultaneously provided a means for determining the inherent pointing resolution of the feed array on the 70-meter antenna. It was discovered that 1 millidegree pointing offsets were detectable at all elevations despite antenna distortion, implying that with some additional interpolation this technique can provide real-time pointing updates with less than a millidegree uncertainty.

Due to lack of time, only a relatively simple, coarse-quantized "least-squares" tracking algorithm could be installed into the DFPA, in order to provide initial information about AFCS "inferred measurement" tracking capabilities under actual operating conditions. This least-squares algorithm tested the real-time observables at 2 mdeg increments in elevation and cross-elevation, and did not employ interpolation to refine its estimates: therefore, it could not be used to fully demonstrate the inherent tracking accuracy of the AFCS. However, recovery from applied offsets and closed-loop tracking was verified on DOY-037 and 038, at elevations of 46, 57 and 73 degrees, using DS1. In each case, the "inferred measurement" least squares algorithm found a stable point, provided updates to the antenna at 20 second intervals, and continued to track the source close to the true peak (with approximately 2 mdeg offset in some cases, as expected due to the rough quantization). Finer quantization in the model and the use of interpolation are expected to reduce these algorithm offsets to less than 1 mdeg uncertainty in future versions.

An example of AFCS recovery and tracking by means of the "inferred measurement" least-squares tracking algorithm is provided in Fig. 5, which is part of the record of the track on DOY-037, at an elevation of 46 degrees. The time axis is in hours past 00 UTC. The AFCS was tracking DS1 using the least squares tracking algorithm, registering 40 dB-Hz SNR in the central channel and about 41 dB-Hz in the combined channel: at approximately 1.885

hrs. UTC the tracking algorithm was stopped and offsets of +6 mdegs in both elevation and cross-elevation were applied, causing a 15 dB drop in central channel, and 5 dB drop in combined channel. After reactivation, the least squares algorithm measured the applied offsets (with 2 mdeg. resolution) and correctly repointed the antenna towards the source, clearly demonstrating SNR recovery. This test was repeated at about 1.915 UTC, this time with ±6 mdeg. offsets, with similarly successful results. Additional tracking experiments carried out on DOY-038 at elevations as high as 73 degrees also resulted in successful tracks, demonstrating the ability of this AFCS "inferred measurement" algorithm to keep the antenna pointed "on-source", even in the presence of severe antenna distortions.

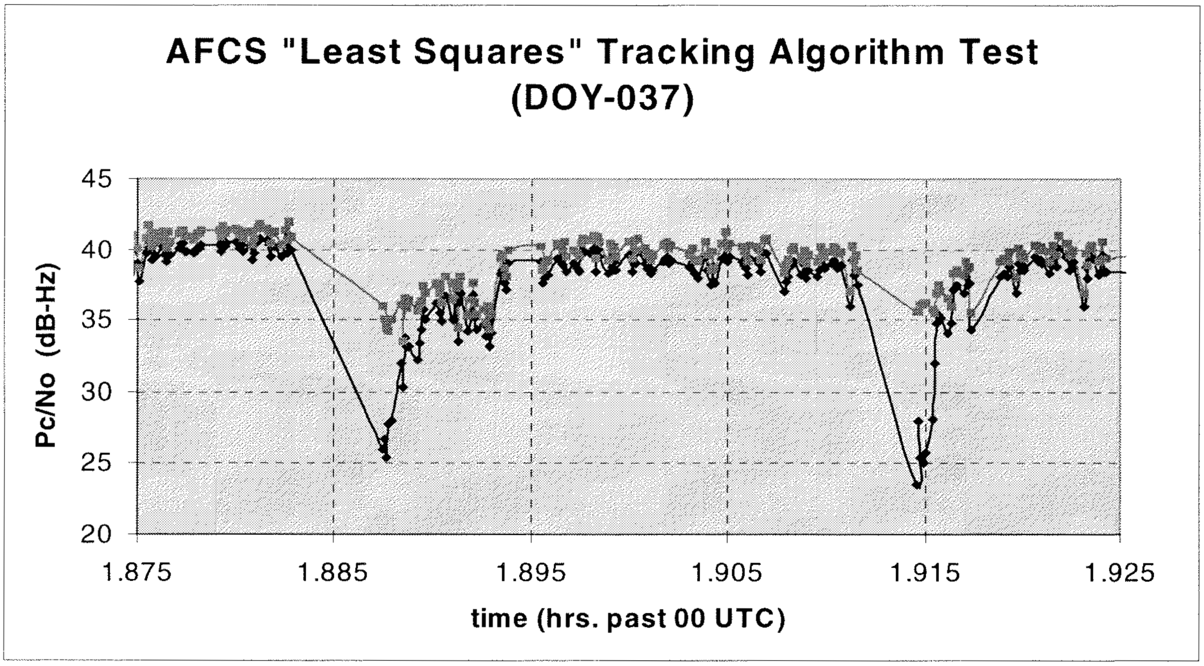

Fig. 5 Pointing Recovery and Tracking of "Least Squares" Tracking Algorithm

JOINT AFCS-DFP MEASUREMENTS

Due to time-constraints on the holography-cone experiments, only the lower range of elevations could be investigated with the joint AFCS/DFP configuration, covering elevations from slightly above the rigging angle (about 50 deg. elevation) down to nearly the software limit of the antenna (8.5 deg.). For this joint configuration, the AFCS front-end was moved from its initial position on the focal-circle looking directly at the subreflector (designated F1), to a new location behind the DFP inside the cone (F2). Apparently the vacuum-seal on the dewar was slightly damaged during the move, because the dewar failed to cool down to cryogenic temperatures after it was moved. Following several failed attempts to cool down the dewar this effort was abandoned, and preparations were made to observe DS1 with a "room temperature" system. Fortunately, due to the proximity of the spacecraft, room temperature operation was a viable option: the strong Ka-band residual-carrier yielded SNR's in excess of 30 dB-Hz near the rigging angle even with room temperature LNA's, which was more than adequate for conducting joint AFCS/DFP compensation experiments.

Three distinct experiments were carried out on DOY-056, while tracking DS1: the peak response of each horn was mapped using direct boresights on each horn; the central and combined channels were supplied to a Block V Receiver (BVR) in SPC-10 for independent combining-gain measurements; and joint AFCS/DFP compensation experiments were carried out as the spacecraft descended towards the horizon. The results of these activities are summarized in the following sections.

1. Mapping of the Array Feed Horns

The horn mapping activity took place between 0324 UTC and 0411 UTC, as the spacecraft continued to ascend from about 70 to 77 degrees elevation. First, two boresights were performed on the central horn (channel 1), the offsets from the predicts noted (these offsets were needed to peak up the source in the new location on the cone), and a digital SNR measurement was made. The antenna was then repointed in the nominal direction of horn #2 and the source located in the second channel by entering manual offsets. The signal was then peaked up using two more boresights on the output of the second horn, and the SNR recorded. This process was repeated for the remaining horns, after which the central horn was remeasured as a consistency check. The results are summarized in Table 1:

Table 1. Mapping the Peak Response of the Seven Array Feed Horns

Horn #	Elevation (deg)	Offsets (mdeg)	SNR (dB)
1	70	(-13.4, 2.6)	30.5
2	71	(- 5.9, 12.5)	29.5
3	72	(- 0.6, 1.6)	32.4
4	73	(- 8.3, - 8.9)	30.0
5	74	(-20.9,- 6.3)	28.6
6	75	(-25.3, 4.6)	29.9
7	76	(-15.9, 14.5)	28.2
1	77	(-11.0, 4.4)	28.6

Note the 2 dB drop in the central channel SNR between the first and last measurements as well as the change in the offsets, due to the higher elevation of the last measurement.

2. Independent Verification of Combining Gain

During most of the holography-cone experiments, combining-gain was measured digitally with the DFPA, using two nearly independent techniques: first, the SNR in each channel was measured and the sum of the channel SNR's computed to obtain an estimate of the combined-channel SNR as indicated by equation (4); next, the actual SNR of the optimally weighted combined channel was measured after application of the estimated real-time combining-weights. In each case, the resulting SNR was divided by the SNR of the central channel to obtain the combining gain estimate. During each track, the results of both measurements were recorded and displayed on the monitor on demand. Typically, both measurements agreed to within a few tenths of a dB, providing mutual confirmation since fundamentally different measurement techniques were employed in the two cases.

In order to further check the validity of these digital measurements, each output channel (central and combined) was upconverted to 300 MHz IF, transmitted to SPC-10 and input to a BVR. The BVR locked up to the residual carrier for either the central or the combined channel (whichever was transmitted), and recorded its own estimate of the signal-to-noise ratio. Since only a single-channel analog upconverter was available, it was decided to incorporate a digital switch into the DSPA, enabling selection of either the central or the combined channel, thus supplying the baseband in-phase and quadrature signals to the upconverter, which then produced a single (real) IF suitable for transmission to the BVR.

For approximately twenty minutes at an elevation of 78 degrees (near transit), the output of the DSPA was switched between the central and combined channels, and the SNR-s measured by the BVR were recorded. The results of this verification experiment are shown in Fig.5: it can be seen that the SNR of the combined channel is close to 29 dB-Hz throughout the experiment, while that of the central channel falls below 26 dB-Hz near the end, indicating a gain of up to 3 dB. These results are consistent with SNR's measured and recorded previously by the DSPA at similar elevations, as shown previously in Fig. 4.

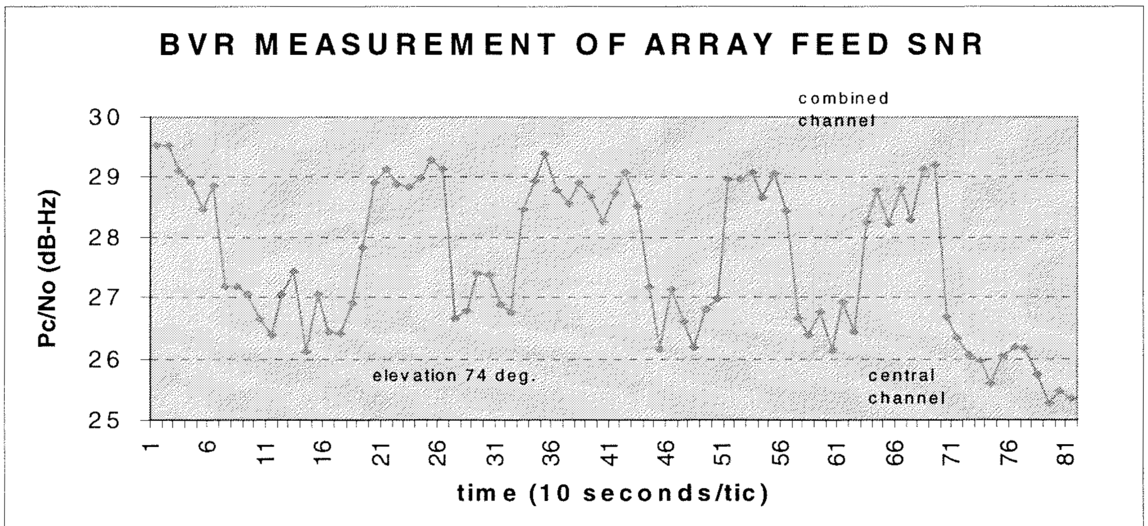

Fig. 6 BVR Measurement of AFCS Central and Combined Channel SNR

Joint AFCS-DFP Compensation Experiment

Analysis of the data obtained on DOY-056 clearly demonstrated that a joint Ka-band AFCS/DFP compensation system working together in real-time could recover virtually all of the signal energy lost to gravitational deformations at intermediate to low elevations, effectively synthesizing an undistorted 70-meter antenna at Ka-band frequencies.

On DOY-056, DS1 was tracked continuously as it descended from an elevation of approximately 50 degrees down to 8.5 degrees. Both BVR and AFCS data were taken simultaneously during the track. With the DFP flat, boresights were performed to center the source in the central channel, after which the DFP was flexed in an attempt to refocus the distorted fields back into the array. Since the data recorded by the BVR is not elevation tagged, only time-tagged, the operator's notes were used to help identify the state of the DFP. The DFP "flat" and "flex" times were confimed using recorded AFCS data, which contains both time and elevation information.

AFCS data collected during this joint track is shown in Fig.7a, where all feed powers were normalized to the signal power in the central channel in order to eliminate the effects of possible variations in signal power: with equal noise power in all of the channels, SNR and signal power are proportional, hence the normalized power of the combined channel is recognized as the combining gain defined earlier in equation (4). Fig. 7b is a logarithmic plot of the same data which better shows the contribution of the outer horns to the total collected signal power as a function of elevation.

The normalized power in all of the outer feeds, as well as the total power, is seen to vary as the state of the DFP changes: when the DFP is flat, the outer feeds contain more power, and when the DFP is flexed the power in the outer feeds is reduced, but not eliminated, as the DFP successfully concentrates some of the distorted signal fields into the central horn. This effect can be clearly seen in Fig. 7a at elevations of 8.5, 13, 16.5, 23, 28 and 33 degrees, becoming less pronounced at the higher elevations. At low elevations the AFCS combining gain is approximately 2 dB when the DFP is flat, but remains slightly above 1 dB even as the DFP is flexed. Results based on analysis of the BVR data is presented in Table 2:

Table 2: Average Combining Gain of AFCS, DFP and AFCS+DFP on DOY-056

Elevation	G_{AFCS}	G_{DFP}	G_{joint}	ΔAFCS	ΔDFP
8.5 deg	2.1 dB	1.8 dB	2.9 dB	1.1 dB	0.8 dB
13	1.8	1.6	2.5	0.9	0.7
16.5	1.6	1.4	2.2	0.8	0.6
23	1.2	1.1	1.8	0.7	0.6
28	1.1	0.9	1.5	0.6	0.4
33	0.75	0.6	1.0	0.3	0.25
38	0.5	0.3	0.6	0.4	0.1

The various gains used in Table 2 are defined as follows: $G_{AFCS} = G_c$ is the array gain over the central channel, as defined in equation (1), when the DFP is flat; G_{DFP} is the increase in signal power in the central channel when the DFP is flexed; G_{joint} is the gain over the uncorrected central channel due to both the DFP and the AFCS operating jointly to recover losses; ΔAFCS is the gain contributed by the AFCS to G_{joint}, over that of the DFP acting alone; ΔDFP is the gain contributed by the DFP to G_{joint}, over that of the AFCS acting alone.

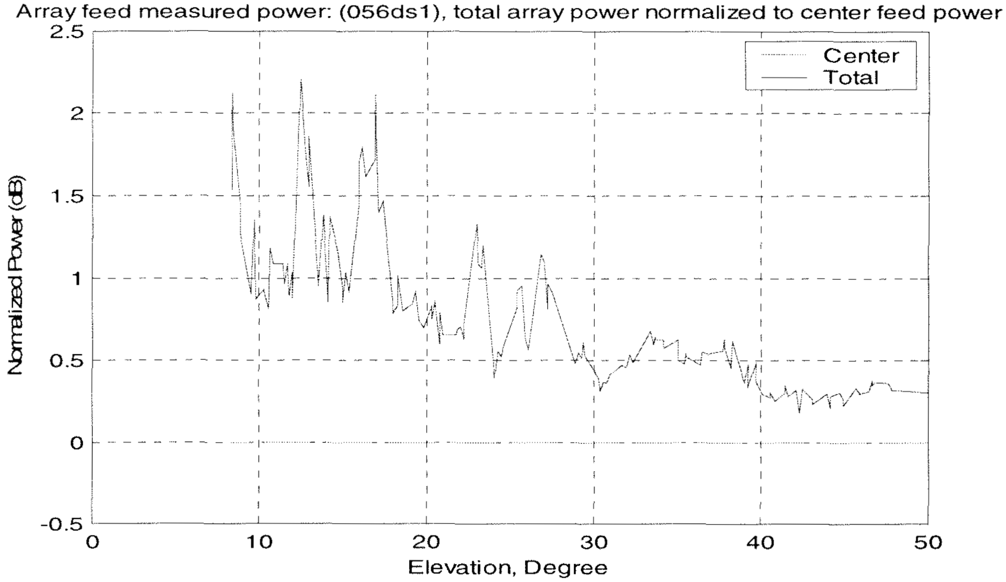

Fig. 7a AFCS data taken during DS1 track on DOY-056 (DFP "flat" and "flexed")

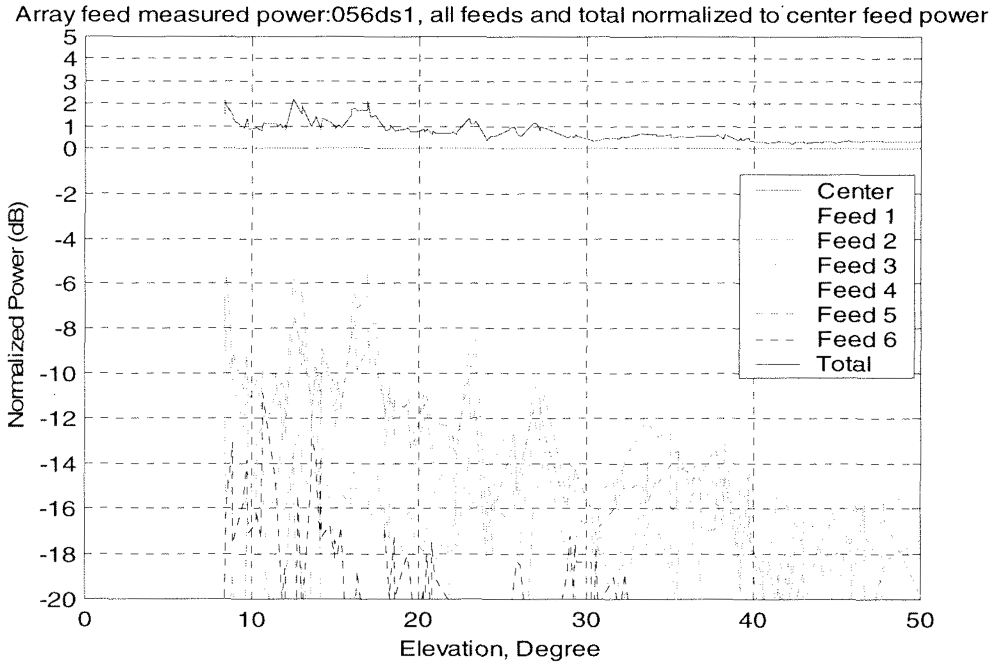

Fig. 7b AFCS data taken during DS1 track on DOY-056 (DFP "flat" and "flexed")

The results tabulated above are also shown in graphical form in Fig. 8, where the measured AFCS gains (in dB) have been added to the SNR measurements recorded by the BVR . It can be concluded that either the AFCS or the DFP acting individually can recover up to 2 dB of SNR at low elevations: however, the combination of the two systems operating jointly yields substantial additional improvements, amounting to more than 1 dB over that of the DFP acting alone

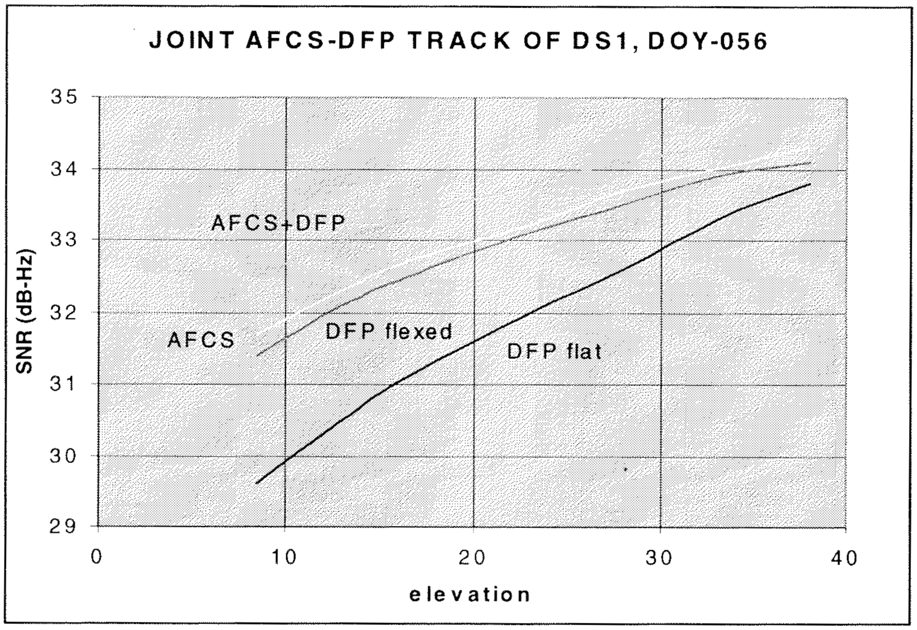

Fig. 8 Results of Joint AFCS+DFP Compensation Experiment

SUMMARY AND CONCLUSIONS

It has been demonstrated that most of the SNR (or efficiency) losses incurred from mechanical antenna distortions can be recovered by means of a properly designed real-time compensation system consisting of a 7-element array feed receiver (AFCS), operating in combination with a deformable flat plate (DFP) designed to redirect divergent rays back into the array. It has been shown that such a combination system recovers approximately 3 dB out of a possible 4 dB at low elevations, and is believed capable of recovering more than 6 dB (out of a possible 8 dB) at high elevations, effectively synthesizing a "flat" antenna response at Ka-band frequencies. This approach has the added advantage of providing simultaneous closed-loop tracking by means of array feed "inferred measurement" tracking algorithms, one of which was successfully demonstrated during the holography cone experiments.

ACKNOWLEDGEMENTS

The authors would like to thank Vahraz Jamnejad for generating the plots in Fig. 7a and 7b.

REFERENCES

1. A. W. Rudge and D. E. N. Davies, "Electronically controllable primary feed for profile error compensation of large parabolic reflectors," *Proceedings of IEEE*, vol. 117, pp. 351-358, 1970.

2. S. J. Blank and W. A. Imbriale, "Array feed synthesis for correction of reflector distortion and vernier beam steering," *TDA Progress Report 42-86*, JPL, pp. 43-55, Aug. 15, 1987.

3. A. R. Cherrete, R. J. Acosta, P. T. Lam, and S. W. Lee, "Compensation of reflector antenna surface distortion using an array feed," IEEE Transactions on Antennas and Propogation, vol. 37, pp. 966-978, Aug. 1989.

4. P. W. Cramer, "Initial studies of array feeds for the 70-meter antenna at 32 GHz," *TDA Progress Report 42-104,* JPL, pp. 50-67, Feb. 15,1991.
5. V. Vilnrotter, E. Rodemich, and S. Dolinar, Jr., Real-time combining of residual carrier array signals using ML weight estimates," *IEEE Transactions on Communications*, vol. 40, pp 604-615, Apr. 1992.

6. V. Vilnrotter, D. Fort and B. Iijima, "Real-time array feed system demonstration at JPL," in *Multifeed Systems for Radio Telescopes*, Astronomical Society of the Pacific Conference Series, vol. 75, pp. 61-73, 1995.

7. K.-M. Cheung and V. Vilnrotter, "Channel capacity of an array system for Gaussian channels with applications to combining and noise cancellation," TDA Progress Report 42-124, JPL, pp. 53-62, Feb. 15, 1996.

8. P. Richter, "Radio Source List for Antenna Calibration," JPL Document # D-3801, DSN # 890-269, Oct. 15, 1994